Energetic neutral particle production
in the cathode sheath of direct-current discharges

Tsuyohito Ito[1], Mark A. Cappelli[2]

[1]*Frontier Research Base for Global Young Researchers, Frontier Research Center*
Graduate School of Engineering, Osaka University, 2-1 Yamadaoka, Suita, Osaka 565-0871, Japan
[2]*Mechanical Engineering Department, Stanford University, Stanford, CA 94305-3032, USA*

Abstract: Direct measurements and Monte Carlo simulations of the energy distribution of energetic neutrals incident onto the cathode of a dc glow discharge are presented. The measurements are performed by time-of-flight analysis of neutrals escaping through a cathode orifice. The experimental results are found to be in good agreement with Monte Carlo simulations. It is found that commonly-used theories for the production of energetic neutrals through charge exchange in the cathode sheath do not capture the neutral energy distribution over the range of discharge voltage studied.

Keywords: Neutral energy distribution, cathode sheath, time-of-flight measurement

1. Introduction

Energetic neutrals formed by collisions with accelerated ions in the sheaths of direct-current (dc) discharges contribute to secondary electron emission, electrode erosion, and discharge gas heating. Although many measurements have been made of the ion energy distribution in dc sheaths and good agreement is seen with theoretical predictions [1-3], with the exception of one preliminary attempt [4], there seems to be no extensive measurements of the energy distribution of neutrals at the cathode in dc discharges. This is despite the availability of various theories [5-8] and computational studies [8-10]. This study presents direct time-of-flight (TOF) measurements of high-energy neutrals impinging on the cathode in argon dc glow discharges. The variation in the energy distribution with discharge voltage is characterized and compared to Monte Carlo simulations. The validities of the simple theoretical predictions are discussed. The results indicate that some theories [5-7] do not adequately describe neutral particle collisions in the cathode sheath, and hence do not capture the neutral energy distribution for a broad range of discharge conditions. Angle dependencies simulated by MC simulation show that scattering should be accounted for in theories for the neutral energy distributions, while the scattering may be less important for ion energy distributions.

2. Experiments

The TOF measurements were made of argon neutrals drifting parallel to the electric field direction, i.e., perpendicular to the cathode of a dc discharge cell, as shown in Fig.1. The abnormal dc glow discharges are generated in pure argon at a pressure of 0.5 Torr with a 6 cm diameter copper cathode, a stainless-steel anode, and an electrode separation of 5 cm. We have collected data for a range of values for the voltage and current shown in Fig.2.
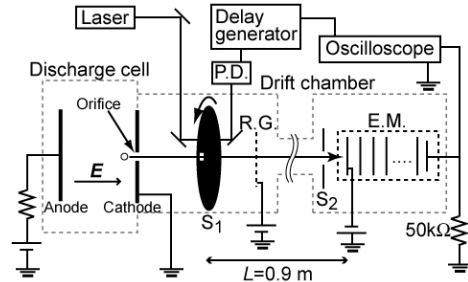

FIG. 1. Schematic of the experimental setup for measuring neutral energy distribution: slit 1 and 2 (S1 and S2), positively biased ion retarding grid (R. G.), photo diode, (P. D.), and electron multiplier (E. M.).
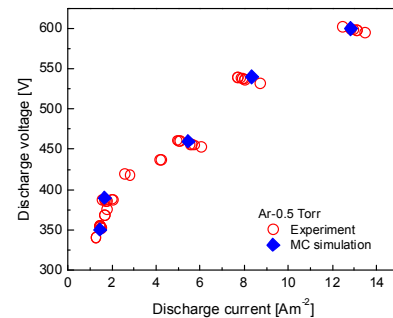

FIG.2 Current-voltage characteristics

Energetic neutrals formed near the cathode by charge exchange collisions with impinging ions are sampled through a 100 μm diameter orifice (~50 μm thick cathode foil). The sampled beam is interrupted by a high-speed (20,000 rpm) chopper, placed 3 cm downstream of the orifice, which contains a single 0.3 mm – wide slit on its blade, 4 centimeters from the rotational axis. The drifting neutral stream impinges onto a 17 stage electron multiplier containing Cu-Be dynodes, located 0.9 m downstream of the chopper. A second (3 mm wide) slit is placed in front of the electron multiplier for improving temporal

response. A positively-biased grid is placed just down-stream of the discharge cathode and the chopper to serve as an ion filter, allowing only neutrals to pass into the drift tube and migrate towards the electron multiplier. It is noteworthy that the solid angle collected by the spectro-meter, as limited by the slit in front of the detector, is ~ 7.5×10^{-5} sr. A He-Ne laser modulated by the same chop-per is used as a timing reference for triggering the oscil-loscope, on which the TOF traces are recorded and aver-aged. The zero-drift time is determined by the signal cor-responding to detected photons from the discharge ob-served with reverse polarity (so that the orifice is now on the anode and there is little or no detected energetic neu-tral signal). The photon signal has a 5 μs rise time with a full-width at half maximum of 5 μs. This signal serves as an indication of the instrument broadening and is used to deconvolve the TOF spectra.

3. Monte Carlo simulations

The MC simulations use a sheath thickness and poten-tial distribution determined from the collisional form of Child's law [11], assuming a constant charge exchange cross section (Q_{ch}) of 4×10^{-19} m^2. Measurements of the ion energy distribution from similar discharges suggest that the charge exchange cross sections should be in the range of $3.7-7.2 \times 10^{-19}$ m^2 [1-3,12,13]. In our MC simu-lations, particles collide in accordance with the ener-gy-dependent collisional cross sections proposed by Phelps et al. [12-14]. Ions are introduced at the sheath edge with random velocities, sampling these velocities from a Maxwellian distribution at the presumed gas tem-perature of 300K. Neutral-neutral collisions are simulated using a hard sphere model with the differential cross sec-tion reported by Phelps et al. [14]. Ion-neutral collisions are simulated by a combination of a charge exchange col-lision model and an isotropic hard sphere model, as pro-posed by Phelps [12, 13]. In treating the charge exchange collision, the incident ion becomes a neutral particle without a change in its velocity while the slow ion pro-duced takes on a random velocity determined by the gas temperature. In reality, the energetic neutral formed in the charge exchange collision may experience small angle scattering, however, to our knowledge, there is no availa-ble differential cross section database for ion-neutral col-lisions. To examine sensitivity of the results to small an-gle scattering, we examine the performance of a model with random scattering angles within a center-of-mass forward scattering angle of 10º.

In comparing to TOF measurements, we consider the particles impinging on the cathode within the solid angle limited by the detector used in the experiments.

4. Results and discussion

Representative experimental (uncorrected) TOF spectra for varying discharge voltage are shown in Fig. 3. The increases in signal intensity and a shift in peak position to shorter drift times with increasing voltage is apparent. The corresponding energy spectra are obtained following deconvolution and correction for the energy dependence of the secondary electron emission of neutral argon on Cu-Be [15]. It is noteworthy that the secondary electron emission can depend on surface conditions, as pointed out by Phelps et al. [16]. We have not pre-treated or cleaned the Cu-Be dynode for these studies, and therefore employ the secondary emission coefficient for untreated (native) Cu-Be surfaces, as reported in Ref. 15. Also shown in Fig. 3 is the 600V case deconvolved for instrument broadening using the photon signal. As seen in the TOF spectra of Fig. 3, there are weak peaks between 0-5 μs and 10-20 μs, the origin of which are attributed to hydrogen and oxygen contamination, perhaps as a result of sputtering of surfac-es within the drift section of the spectrometer. These peaks were not sensitive to Ar flow rate and there was only weak optical emission associated with hydrogen, and no emission due to oxygen, from the discharge itself, re-ducing the likelihood that this contamination originates in the discharge. These interferences precluded energy mea-surements beyond an energy of approximately 200 eV for the lowest discharge voltage case (350V), and about 500 eV for the highest discharge voltage (600V). Operation of the discharge on helium confirmed that there is no conta-mination from heavier species that might overlap with the argon signal at lower energy.

Figure 4 shows the converted neutral energy spectra (lines) along with the results of MC simulations (symbols: for neutrals scattered over limited angles). The variation in neutral energy distribution with discharge voltage is apparent, with a higher discharge voltage resulting in a more energetic high energy tail. The agreement between experiments and MC simulations is remarkable. In par-ticular, it is noteworthy that the relative intensity with varying voltage for either the predicted or measured dis-tributions is not adjusted once the experimental distribu-tion for the 350V case is scaled to overlap with that simu-
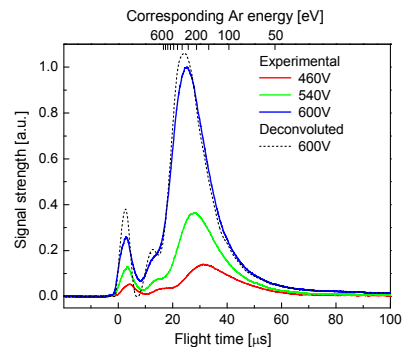
FIG. 3. Observed time of flight spectra for a range of discharge voltage and deconvolved spectrum for 600V. TOF signals are normalized by the maximum value of the spectra for the 600V discharge case.

lated. Note that the input to the MC simulations does include both the experimental discharge current and the discharge voltage, and so this relative agreement is not unexpected.

The distributions have been compared to those predicted by simple theories [5-7]. As the simple theories do not account for the possibility of scattering into a range of angles, we compare the energy distributions to those predicted by MC simulations with neutrals scattered into all possible angles. This comparison is made in Fig. 5. Also included in this figure is the theoretical and simulated ion energy distribution. The values in the index are ratios of the so-called cross section for stopping neutrals by neutral-neutral collisions (Q_s) to the cross section for ion-neutral charge exchange, $Q_{ch}, (= 4 \times 10^{-19} \text{ m}^2)$ [7]. Q_s represents the probability that a neutral collision occurs, resulting in a total loss of forward momentum. A value of zero for this ratio implies that all high energy neutrals created by charge exchange collisions arrive at the cathode without further energy loss, in accordance with the approach of Abril et al. [5,6] We see that a value of Q_s/Q_{ch} = 0.5-0.7 seems to lead to a similar distribution predicted by the MC simulations (considering all angles), even though this theory does not account for scattering into shallow angles or energy exchange between neutrals by collisions. However, while this value provides agreement for the 350V discharge case, a new value for this cross section ratio is found to be needed to obtain agreement at other discharge voltage conditions, i.e., there is no unique ratio of Q_s/Q_{ch} that captures the trends seen in all of the experiments, pointing to inadequacies in this simple theoretical description [5-7]. The theory by Hagelaar et al. [8], which derived the highest and lowest limits for the neutral energy distributions through a rate equation based on a local field model, is not considered in this study, since the use of a local field model may not be suitable for computing energy distributions in the cathode sheath (except perhaps for the very low energy portion of the ion energy distributions), where the electric field variation is significant.
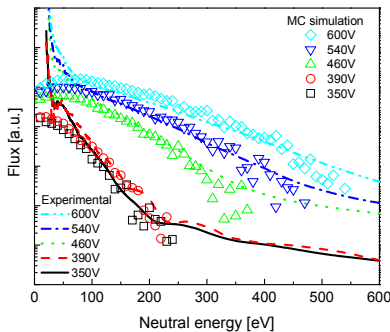

FIG. 5. Representative MC simulations and theoretical predictions (Refs. 1, 2, and 5-7) of ion and neutral energy distributions, and the measured neutral energy distribution (0.5 Torr, 350V, and 1.4Am^{-2}).

We speculate that the main reason that the simple theories fail to capture the trends in the neutral energy distributions for the wide range of operating conditions is the failure to account for the partitioning of energy amongst the two collision partners and also the angular scattering that arises. Figure 6 shows particle distributions (particle flux per unit solid angle) as functions of energy and scattering angle. We can see that ions (top panel) are dominantly scattered into a very narrow angle, since charge exchange collisions are dominant and ions are accelerated by the electric field. In contrast, neutrals (bottom panel) are scattered into a wider range of angles. The broadening in the neutral distributions arises in part because the high energy neutrals generated by charge exchange collisions are no longer accelerated and can create other high-energy neutrals at new scattering angles by subsequent collisions. In the MC simulation results described above, the modeling of the charge exchange collisions did not alter the

FIG.4 Measured (thick lines) and MC simulations (symbols) of the neutral argon energy distribution. Both the measured and simulated distributions are for neutral atoms sampled over the limited detection angle of the experiment.
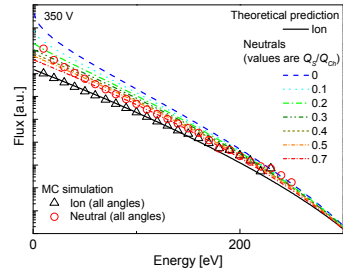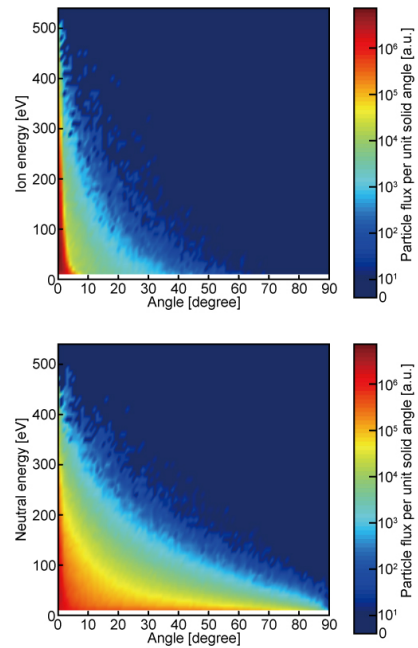

FIG. 6. Particles flux map as functions of scattering angle and particles energy for 540V and 8.3Am^{-2}: ions (top panel) and neutrals (bottom panel).

trajectories of the particles. As a result, the angular distribution of the high-energy neutrals originate as a result of the initial ion velocities (sampled from a Maxwellian distribution at 300K or scattered by isotropic collisions, and then altered by the applied field) and from neutral-neutral scattering events.

While reasonable agreement is obtained between the simulated neutral energy distributions and those predicted using the MC simulations, as seen in Fig. 4, improved agreement can be obtained, especially at lower energy, by including angular scattering in the charge exchange collisions. As mentioned earlier, this requires knowledge of the differential cross section for ion-neutral scattering collisions. Since there seems to be no available differential cross section data for argon ion-neutral collisions, we have examined the effect of differential (angular) scattering in our charge exchange collision model by assuming that charge exchange collisions occur with random-angle scattering within 10º in the center-of-mass flame. Figure 7 presents the results of this revised MC simulation along with the experimental TOF data. We find that the flux is lower (at all energies) than that predicted in the absence of angular scattering (the comparison is not shown here). Adding angular scattering events into the charge exchange collision model decreases the high energy flux more than the flux at low energies, resulting higher relative flux at low energy. Overall, it appears that there is still very reasonable agreement (perhaps slightly better) with experimental data, although it is apparent that additional experimental results are needed to further examine the importance of angular scattering in charge exchange collisions, as is fundamental data on differential scattering for charge exchange processes. It is noteworthy that the energy distribution resulting from integration over all angles is altered only negligibly.

These results confirm the importance of direct measurements of neutral energy distributions, such as the TOF experiments of the type reported, in understanding complex collisional processes in the sheaths of direct current discharges. More refined experiments combined with MC simulations can be useful in testing collisional models.
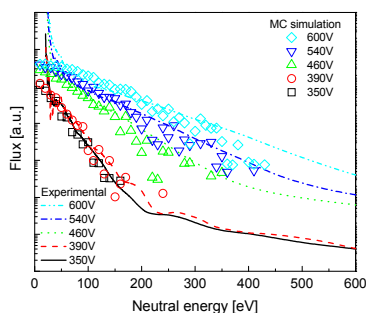

FIG.7 Measured (thick lines) and MC simulations (symbols) of the neutral argon energy distribution with small-angle scatterings in a charge exchange collision model.

5. Summary

This study represents the direct measurement and the MC simulation of the energy distribution of neutral particles incident onto the cathode of a dc glow discharge. The measurements are in good agreement with MC simulations, although in both cases, the forward angle of the neutrals considered or sampled in the experiments are limited to the corresponding solid angle of detection by the TOF spectrometer. While simple theories using constant cross sections for charge exchange and forward momentum loss collisions provide some agreement with experiments over a limited range of conditions, these theories do not provide agreement over a broad range of conditions. A preliminary sensitivity of the MC simulations to angular scattering in ion-neutral collisions suggests that improved agreement can be obtained by including more complex modeling of the charge exchange collision processes.

References
1. W. D. Davis and T. A. Vanderslice, Phys. Rev. 131, 219 (1963).
2. C. V. Budtz-Jørgensen, J. Bøttiger, and P. Kringhøj, Vacuum 56, 9 (2003).
3. T. Ito and M. A. Cappelli, Phys. Rev. E, 73, 046401 (2006).
4. D. G. Armour, H. Valisadeh, F. A. H. Soliman, and G. Carter, Vacuum 34, 295 (1984).
5. I. Abril, A. Gras-Marti, and J. A. Vallés-Abarca, Phys. Rev. A 28, 3677 (1983).
6. I. Abril, A. Gras-Marti, and J. A. Vallés-Abarca, J. Phys. D: Appl. Phys. 17, 1841 (1984).
7. R. S. Mason and R. M. Allott, J. Phys. D: Appl. Phys. 27, 2372 (1994).
8. G. J. M. Hagelaar, G. M. W. Kroesen, and M. H. Klein, J. Appl. Phys. 88, 2240 (2000).
9. V. V. Serikov and K. Nanbu, J. Appl. Phys. 82, 5948 (1997).
10. I. Revel, L. C. Pitchford, and J. P. Boeuf, J. Appl. Phys. 88, 2234 (2000).
11. M. A. Lieberman and A. J. Lichtenberg, Principles of plasma discharges and materials processing. New York: Wiley, 1994. p. 170.
12. A. V. Phelps, J. Appl. Phys. 76, 747 (1994).
13. A. V. Phelps, private communication. ftp://jila.cololado.edu/collision_data/.
14. A. V. Phelps, C. H. Green, and J. P. Burke Jr., J. Phys. B: At. Mol. Opt. Phys. 33, 2965 (2000).
15. K. Kadota and Y. Kaneko, Jpn. J. Appl. Phys. 13, 1554 (1974).
16. A. V. Phelps and Z. Lj. Petrović, Plasma Sources Sci. Technol. 8, R21 (1999).